PERGAMON

Chemical Engineering Science 57 (2002) 4161–4171

Chemical Engineering Science

www.elsevier.com/locate/ces

Miniature free-piston homogeneous charge compression ignition engine-compressor concept—Part I: performance estimation and design considerations unique to small dimensions

H. T. Aichlmayr, D. B. Kittelson, M. R. Zachariah *

Departments of Mechanical Engineering and Chemistry, The University of Minnesota, 111 Church St. SE, Minneapolis, MN 55455, USA

Received 18 September 2001; received in revised form 7 February 2002; accepted 18 April 2002

Abstract

Research and development activities pertaining to the development of a 10 W, homogeneous charge compression ignition free-piston engine-compressor are presented. Emphasis is placed upon the miniature engine concept and design rationale. Also, a crankcase-scavenged, two-stroke engine performance estimation method (slider-crank piston motion) is developed and used to explore the influence of engine operating conditions and geometric parameters on power density and establish plausible design conditions. The minimization of small-scale effects such as enhanced heat transfer, is also explored.
© 2002 Published by Elsevier Science Ltd.

Keywords: Two-stroke engine; Free-piston engine; Homogeneous charge compression ignition; Microchemical; Performance estimation; Micro-power generation

1. Introduction

This paper is the first in a two-part series that presents results of recent small-scale engine research and development efforts conducted at the University of Minnesota. Specifically, it introduces the miniature free-piston homogeneous charge compression ignition (HCCI) engine-compressor concept, explores possible operating conditions and constraints, establishes potential engine configurations, and identifies design considerations peculiar to miniature engines. It does not, however, address details of the HCCI combustion process; this is left to the second paper.

1.1. Micro-power generation

Considerable efforts have been directed toward enhancing portable electronic devices, yet their primary power source i.e., batteries, remain essentially unchanged. Batteries enable one to take these devices virtually anywhere, but their intrinsically low energy densities and short lifetimes impose a fundamental limitation. To mitigate it, only two options exist: Enhance batteries or develop miniature energy conversion devices. Only modest gains may be expected from the former, consequently the latter is being vigorously pursued (Peterson, 2001). In particular, miniature engine-generators (Epstein et al., 1997; Yang et al. 1999; Allen et al., 2001; Fernandez-Pello, Liepmann, & Pisano, 2001) are considered especially promising.

At first glance, replacing batteries with miniature engine-generators appears to be an absurd proposition. Consider however, the enormous energy densities of hydrocarbon fuels e.g., 46 MJ/kg. In contrast, the energy density of premium lithium batteries is approximately 1 MJ/kg (Yang et al., 1999). Therefore, an engine-generator having a fuel conversion efficiency of only 2.5% would out-perform any battery. Of note, the fuel conversion efficiency of the smallest commercially available model airplane engine (Cox 0.010) is approximately 4% (Yang, 2000). Hence this proposition is sensible.

1.2. Micro-combustion

Despite the clear advantage that a miniature engine-generator has relative to a battery, significant technical obstacles exist. Some of which include: (1) micro-combustion,

* Corresponding author. Tel.: +1-612-626-9081; fax: +1-612-625-6069.
E-mail address: mrz@me.umn.edu (M. R. Zachariah).

0009-2509/02/$ - see front matter © 2002 Published by Elsevier Science Ltd.
PII: S0009-2509(02)00256-7

(2) thermal management, (3) gas exchange, (4) friction, (5) sealing, and (6) materials and fabrication limitations. Thus far, work at the University of Minnesota has focused upon micro-combustion.

Micro-combustion could be influenced by substantial heat and mass transfer to the boundaries. To illustrate, consider the specific heat transfer rate from a stagnant gas occupying a chamber having a volume $\tilde{V}$ and surface area A_s. If one further considers an average heat flux and density, then the specific heat transfer rate defined by

$$\dot{q} = \frac{\dot{Q}}{m} = \frac{\int_{A_s} \dot{q}'' \, \mathrm{d}A}{\int_{\tilde{V}} \rho \, \mathrm{d}V} = \frac{\bar{\dot{q}}''}{\bar{\rho}} \left(\frac{A_s}{\tilde{V}} \right), \tag{1}$$

increases with the surface-area-to-volume ratio, $A_s/\tilde{V}$. The surface-area-to-volume ratio meanwhile, is inversely proportional to the characteristic dimension of the chamber. Thus, the specific heat transfer rate increases when the characteristic dimension decreases.

The phenomenon demonstrated by Eq. (1) is advantageous in micro-chemical systems (Jensen, 1999) because highly exothermic processes such as catalytic partial-oxidation reactions (Srinivasan et al., 1997; Hsing, Srinivasan, Harold, Jensen, & Schmidt, 2000; Quiram, Hsing, Franz, Jensen, & Schmidt, 2000; Quiram et al., 1998) and the catalytic oxidation of H_2 (Hagendorf, Janicke, Schüth, Schubert, & Fichtner, 1998) can be controlled. Conversely, this is a disadvantage if one wishes to minimize heat loss e.g., from a flame, in a micro-sized chamber.

1.3. Micro-internal combustion engines

Several miniature engine programs are underway. Epstein et al. (1997), for instance, are developing a Micro-Gas Turbine Engine at the Massachusetts Institute of Technology. Honeywell International (Yang et al., 1999) is pursuing a 10 W, free-piston homogeneous charge compression ignition (HCCI) engine-compressor. Similarly, Allen et al. (2001) are developing a free-piston spark ignition (SI) engine-generator at the Georgia Institute of Technology. Alternatively, a MEMS rotary engine (Fernandez-Pello et al., 2001) is under development at The University of California, Berkeley.

Although each of the aforementioned micro-engine programs have unique advantages and disadvantages, they share a common problem: flame quenching. Each engine proposal may then be characterized according to their solution: Waitz, Gauba, & Tzeng, 1998 exploit the unique burning properties of hydrogen and plan to burn hydrocarbons with the assistance of a catalyst; Disseau et al. (2000) employ several miniature spark plugs to maximize the amount of charge consumed before quenching occurs; and Knobloch et al. (2000) reduce quenching effects by heating the walls. Yang et al. propose a novel solution: HCCI combustion.

1.4. Homogeneous charge compression ignition combustion

Homogeneous charge compression ignition (HCCI) combustion is an alternative engine combustion mode first identified by Onishi, Jo, Shoda, Jo, & Kato, (1979). Briefly, HCCI entails compressing a fuel–air mixture until an explosion occurs. It differs from Diesel combustion because the fresh charge is premixed and it differs from SI combustion because the charge auto-ignites. Consequently, HCCI has the following experimentally verified (Iida, 1994; Lavy, Duret, Habert, Esterlingot, & Gentili, 1996; Gentili, Frigo, Tognotti, Patrice, & Lavy, 1997) characteristics: (1) ignition occurs simultaneously at numerous locations within the combustion chamber, (2) an absence of traditional flame propagation, (3) the charge is consumed very rapidly, and (4) ignition is not initiated by an external event.

Although HCCI is a relatively recent research topic, the rudiments of HCCI are well known. That is, HCCI is a form of "knock" combustion and therefore its occurrence depends upon chemical kinetics and the compression process (Najt & Foster, 1983). Knock combustion is typically associated with SI engines and occurs when a pocket of unreacted charge i.e., the end gas, auto-ignites before being consumed by an advancing flame front. When this happens, the end gas burns very rapidly and causes the local pressure to rise violently. This in turn, generates pressure waves that transit the combustion chamber and initiate phenomena that ultimately damage engine components. Consequently, avoiding knock is a basic design constraint for SI engines and despite considerable research efforts (Oppenheim, 1984), it is generally satisfied by restricting compression ratios to modest values e.g., 9:1. Unfortunately, constraining the compression ratio also limits the fuel conversion efficiency.

While knock combustion is generally avoided, it has advantages over more traditional engine combustion modes. Some of which include: (1) the capability to burn extremely lean mixtures, (2) no compression ratio limitation, (3) no external ignition system, (4) unrestricted air intake, and (5) a wide variety of fuels may be used. Burning extremely lean mixtures ($\Phi < 0.5$) is presently the most appealing feature because the resulting low combustion temperatures yield small NO_x emissions. This benefit, however, disappears when the mixture strength is increased (Stanglmaier & Roberts, 1999). Additionally, low combustion temperatures yield relatively large emissions of unburned hydrocarbons and carbon monoxide. Nonetheless, HCCI remains attractive because the combination of lean mixtures, unthrottled air intake, and large compression ratios promise engines with "Diesel-like" fuel economy (Thring, 1989) and small NO_x emissions.

Although promising, HCCI is presently impractical. The chief impediment is ignition control—a requirement shared by any engine that employs a reciprocating piston. Note that in spark ignition and Diesel engines, ignition control is achieved by firing a spark plug and injecting fuel, respectively. Neither technique, however, is applicable to HCCI. Hence one must resort to indirect methods i.e., those which alter the compression process or the fuel oxidation kinetics. Consequently, much work has been directed toward devising and evaluating control schemes (Najt & Foster, 1983; Thring, 1989; Ryan & Callahan, 1996; Aoyama, Hattori, & Mizuta, 1996; Christensen, Johansson, & Einwall, 1997; Gray & Ryan, 1997; Christensen & Johansson, 1998; Christensen, Johansson, AmnJus, & Mauss, 1998; Iwabuchi, Kawai, Shoji, & Takeda, 1999; Christensen & Johansson, 1999; Hultqvist et al., 1999; Richter, Franke, Alden, Hultqvist, & Johansson, 1999; Christensen, Hultqvist, & Johansson, 1999; Flowers et al., 2000; Chen, Konno, Oguma, & Yani, 2000). Of note, ignition control is somewhat less of a problem for two-stroke engines due to incomplete gas exchange (Gentili et al., 1997).

In addition, crankshaft-equipped engines have a feature which exacerbates the ignition control problem: a fixed compression ratio. Hence ignition timing is usually adjusted with pre-conditioning techniques such as varying the charge composition or temperature. These techniques, however, have the disadvantages that HCCI is very sensitive to them and that they can be difficult to implement. In light of these difficulties, alternative engine configurations such as the free-piston, are being explored (Van Blarigan, Paradiso, & Goldsborough, 1998; Goldsborough & Van Blarigan, 1999; Galileo Research Inc., 2001). These engines feature a mechanically unconstrained piston and hence a variable compression ratio. The advantage of an HCCI-variable compression ratio engine configuration is discussed in the second paper.

1.5. *Why HCCI in a miniature engine?*

In the context of conventional engines, HCCI is pursued because NO_x emissions can be dramatically reduced. Therefore, assuming that other regulated emissions requirements—hydrocarbons in particular—can be met and that control problems can be resolved, HCCI is an appealing means to comply with stringent future emissions regulations. In the context of *miniature engines*, however, the most important attributes of HCCI are that the charge is burned essentially without flame propagation and that an external ignition system is not required. Furthermore, auto-ignition implies that the charge is consumed both rapidly and uniformly—much like the SI scheme employed by Disseau et al. (2000). Consequently, quenching effects are minimized without resorting to complicated ignition schemes.

HCCI offers another benefit to miniature engines: a combustion rate essentially limited by kinetics rather than transport. Therefore, HCCI engine operational speeds may far exceed those of conventional engines. This is a crucial result because operating speeds scale inversely with size when other variables are fixed. Hence HCCI promises very small engine sizes; this topic is further investigated in the second paper.

2. A miniature free-piston HCCI engine-compressor

Originally based upon the MEMS Free-Piston Knock Engine (Yang et al., 1999; Yang, Bonne, & Johnson, 2001), the miniature free-piston HCCI engine-compressor concept that is the subject of this work is depicted in Fig. 1. The salient feature of this engine is a mechanically unconstrained piston. Therefore, in contrast to a crankshaft-equipped engine, reciprocating motion is the result of gas pressure acting on the piston.

To illustrate, a force balance (Fig. 1(c)) on the piston gives

$$\sum F_x = m_p \frac{\mathrm{d}^2 x}{\mathrm{d}t^2} = A_C P_C - A_{sc} P_{sc} - A_{cp} P_{cp} - A_B P_B, \quad (2)$$

which couples the piston motion to the states of the gases occupying the combustion and bounce chambers, the scavenge pump, and the compressor. Thus free-piston motion is the result of a "thermodynamic–dynamic balance" (Oppenheim & London, 1950). Also note that because the gas pressures in Eq. (2) depend upon the piston position, Eq. (2) is akin to a differential equation describing a spring–mass system. Consequently, free-piston engines are nominally constant-speed machines whose oscillation frequency is determined by the piston mass and mean gas pressures.

Another prominent feature of free-piston engines is that they execute a two-stroke cycle i.e., each expansion stroke is a power stroke. This is a necessary requirement because the combustion chamber pressure P_C, must increase during the compression stroke (Fig. 1(b)) and the bounce chamber pressure P_B, must increase during the expansion stroke (Fig. 1(a)) to maintain reciprocating motion. A consequence of employing a two-stroke cycle is that a scavenge pump (Fig. 1(a)) is required to force the fresh charge into the combustion chamber. Lastly, the air compressor is used to extract energy from the piston.

3. Two-stroke engine performance estimation

Thus far, features of the miniature free-piston HCCI engine-compressor have been presented, but specific engine dimensions and operating speeds required to deliver 10 W have not. To provide these details and explore the influence of various geometric parameters, a two-stroke engine performance estimation method is developed.

One should note that although a free-piston engine configuration is the ultimate objective, we assume a crankshaft-engine configuration in the following analysis. This simplification is imposed because an expression like Eq. (2) is necessary to determine basic operating parameters such as the engine speed in a free-piston engine.

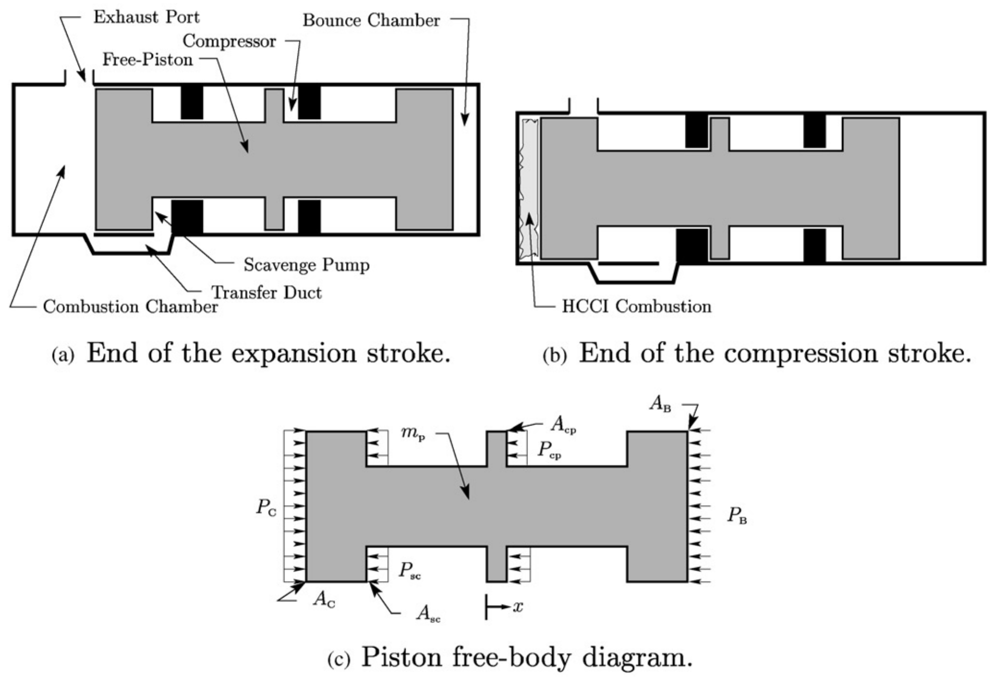

Fig. 1. Miniature free-piston engine concept (intake, compressed air outlet, and counter balance mechanism omitted). (a) End of the expansion stroke; (b) end of the compression stroke; (c) piston free-body diagram.

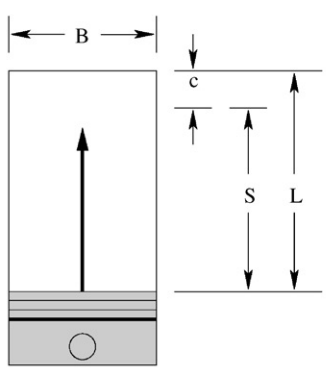

Fig. 2. Single cylinder engine geometry assumed in the performance analysis.

Unfortunately, to use an expression like Eq. (2), many ancillary details e.g., the piston geometry and mass, bounce chamber pressure, and air compressor and scavenge pump performance are required. Such a model would therefore be complicated and generally inappropriate for preliminary work.

3.1. Performance estimation

Consider a single-cylinder, two-stroke, crankcase-scavenged engine having the geometry depicted in Fig. 2. The power delivered P, is given by

$$P = \dot{m}_f e_c \eta_{fc}, \tag{3}$$

where $\dot{m}_f$ is the mass flow rate of fuel, e_c is its lower heating value, and η_{fc} is the fuel conversion efficiency.

The fuel conversion efficiency is defined by Eq. (3) and accounts for various thermodynamic limitations and dissipative effects. Consequently, it is an aggregate quantity and it is usually considered to be the product of: (1) the indicated fuel conversion efficiency, $\eta_{fc,i}$, (2) the mechanical efficiency, η_m, and (3) the charging efficiency, η_{ch}. The indicated fuel conversion efficiency is the thermal efficiency of the engine cycle, or historically, that which one would obtain from an experimental P–V diagram. Hence the indicated fuel conversion efficiency is a measure of how well chemical energy is converted to work. Similarly, the mechanical efficiency accounts for dissipation in mechanical components. While the charging efficiency is a measure of how well the combustion chamber is replenished with fresh charge i.e., the fuel–air mixture. Consequently, it depends upon the gas exchange process and it is therefore strongly related to operating conditions, scavenge port design, and scavenge pump efficiency.

Next, the mass flow rate of fuel is replaced with the product of the mass flow rate of air and the mass-based fuel–air ratio. The fuel–air ratio is subsequently replaced by the product of the equivalence ratio Φ, and the stoichiometric fuel–air ratio F_s. The result is

$$\dot{m}_f = \dot{m}_a F_s \Phi. \tag{4}$$

Similarly, the mass flow rate of air is related to the gas exchange process through

$$\dot{m}_a = N \rho_i V_d \eta_{\text{ch}}, \tag{5}$$

where N is the engine speed, ρ_i is the intake air density, and V_d is the swept volume of the cylinder. Here the charging efficiency is defined to be the ratio of the actual mass of air inducted to the mass of air that the cylinder could contain at ambient conditions. Of note, this assumption results in the charging and volumetric efficiencies being identical (Heywood & Sher, 1999).

The engine speed, however, is not a free variable. Instead, the engine speed and the stroke S, are related through the mean piston speed (Heywood, 1988):

$$\bar{U}_p = 2SN. \tag{6}$$

According to Heywood, the mean piston speed is an indicator of how well an engine handles loads such as friction, inertia, and gas flow resistance. Data from a wide variety of engines operating at rated conditions reveals that the mean piston speed is nearly invariant. Consequently, the mean piston speed is essentially a physical limitation and the operating speed thus depends upon the stroke. But one should note that in a free-piston configuration, the relationship between engine speed, operating conditions, and design parameters is much more complicated.

Next, Eqs. (5) and (6) are related to the cylinder geometry with the stroke-to-bore aspect ratio:

$$R = \frac{S}{B}, \tag{7}$$

the definition of the displaced cylinder volume:

$$V_d = \frac{\pi}{4} B^2 S = \frac{\pi S^3}{4R^2}, \tag{8}$$

the definition of the compression ratio:

$$r = \frac{V_t}{V_c} \tag{9}$$

and the relationship between the total and displaced volumes given by

$$\frac{V_d}{V_t} = \frac{r-1}{r}. \tag{10}$$

Substitution of Eqs. (7)–(10) into Eqs. (3)–(6) and replacing the fuel conversion efficiency with the product of the indicated fuel conversion, mechanical, and charging efficiencies i.e., $\eta_{fc} = \eta_{fc,i}\eta_m\eta_{\mathrm{ch}}$, yields

$$P = \rho_i \frac{\bar{U}_p}{2}\left(\frac{\pi}{4}\right)^{1/3}\left\{\frac{(r-1)V_t}{rR}\right\}^{2/3}\eta_{\mathrm{ch}}\eta_{fc,i}\eta_m F_s \Phi e_c. \tag{11}$$

Also, the engine speed is obtained by manipulating Eqs. (6), (8) and (10) to give

$$N = \frac{\bar{U}_p}{2}\left(\frac{\pi}{4}\right)^{1/3} R^{-2/3}\left\{\frac{(r-1)}{r}V_t\right\}^{-1/3}. \tag{12}$$

3.2. Performance estimation assumptions

The remaining task is to obtain judicious values for the mean piston speed and the various efficiencies. First, the mean piston speed and mechanical efficiency are assumed fixed. Heywood reports that mean piston speeds typically range from 8 to 15 m/s; thus 10 m/s is a reasonable choice. Moreover, the mechanical efficiency is assumed to be 70%.

Second, the indicated fuel conversion efficiency depends upon the compression ratio, the combustion process, the equivalence ratio, and heat transfer to the cylinder walls. Of these dependencies, only the compression ratio dependence is considered here. This dependency is approximately captured by defining an adjusted air-standard Otto cycle efficiency viz.,

$$\eta_{fc,i} = \alpha\{1 - r^{(1-\gamma)}\}, \tag{13}$$

where γ is a mean specific heat ratio and α is an adjustment factor. A reasonable value for α is 0.6 (Taylor, 1985) and $\gamma = 1.3$ is assumed. Other factors that affect the indicated fuel conversion efficiency may be appreciable. Consequently, they are investigated in the second paper.

Next, consider the charging efficiency. This parameter depends upon the mass of fresh charge delivered to the combustion chamber by the scavenge pump and the fraction of the delivered charge that is retained in the combustion chamber. These dependencies are captured by the delivery ratio Λ, and the trapping efficiency η_{tr}; hence $\eta_{\mathrm{ch}} = \Lambda\eta_{\mathrm{tr}}$. Unfortunately, both parameters depend strongly upon the engine design. Consequently, they are impossible to determine a priori.

Fortunately, physical bounds exist for the charging efficiency (Heywood & Sher, 1999). For instance, if the fresh charge completely displaces the exhaust gas, then the charging efficiency and the delivery ratio are identical i.e., $\eta_{\mathrm{ch}} = \Lambda$. On the other hand, if the fresh charge completely mixes with the exhaust, then the charging efficiency is

$$\eta_{\mathrm{ch}} = 1 - \mathrm{e}^{-\Lambda}. \tag{14}$$

These extremes represent maximum and minimum bounds for the charging efficiency. Consequently, the arithmetic mean of these extremes is a reasonable approximation.

Lastly, the charging efficiency depends upon the delivery ratio. Taylor (1985) gives

$$\Lambda = \left(\frac{N_s}{N}\right)\left(\frac{D_s}{V_t}\right)\left(\frac{P_1}{P_e}\right)\left(\frac{T_i}{T_1}\right)\eta_{v,s}, \tag{15}$$

where N_s, D_s, P_1, P_i, T_i, T_1, and $\eta_{v,s}$ are the scavenging pump speed, scavenging pump displacement volume, transfer port pressure, exhaust port pressure, intake temperature, transfer port temperature, and the volumetric efficiency of the scavenging pump, respectively.

Typically, the delivery ratio is found experimentally for a particular engine design and operating condition. Consequently, scavenge pump performance data is scarce. But for a non-supercharged, crankcase-scavenged two-stroke engine, Taylor recommends $N_s/N = 1$, $P_1/P_e \approx 1$, and $\eta_{v,s} = 0.5$. Also, the quantity D_s/V_t is approximated by Eq. (10) and $T_i/T_1 \approx 1$. Under these assumptions, Eq. (15) reduces to

$$\Lambda = \left(\frac{r-1}{r}\right)\eta_{v,s} \tag{16}$$

which completes the necessary set of equations and assumptions for performance estimation.

Table 1
Sample cylinder bores for $P_i = 1$ atm, $T_i = 300$ K and $\Phi = 0.5$ (propane is the fuel)

Compression ratio, r	Cylinder bore, B (mm)	Power output (W)
5	4.97	10
10	4.13	10
20	3.70	10
30	3.53	10
5	1.57	1
10	1.31	1
20	1.17	1
30	1.12	1

4. Miniature engine design

4.1. Engine characteristic dimension and compression ratio

The method developed in the previous section may now be used to obtain specific estimates for the size and operating speed of a 10 W engine. Before proceeding however, consider Eq. (11). This equation implies that P depends upon T_i, P_i, Φ, V_t, r, R, $\bar{U}_p$, η_{ch}, $\eta_{fc,i}$, η_m, e_c, and F_s when $\rho_i = \rho_i(T_i, P_i)$ is assumed. Characterizing this function in terms of all 11 parameters however, is an intractable problem. Consequently the independent variables are grouped into: "intake conditions" (T_i, P_i, Φ), "fuel" (e_c, F_s), and "engine design" $(\bar{U}_p, V_t, r, R, \eta_{\mathrm{ch}}, \eta_{fc,i}, \eta_m)$. The parameter space may be further reduced by fixing the power output, operating conditions, mechanical efficiency, and mean piston speed. Finally, propane is assumed to be the fuel throughout this paper. Under these constraints, Eq. (11) reduces to

$$B^2 \eta_{\mathrm{ch}} \eta_{fc,i} = \frac{8P}{\pi \eta_m F_s e_c \rho_i \Phi \bar{U}_p} = \text{Const.}, \qquad (17)$$

where Eqs. (7), (8), and (10) were used to eliminate the aspect ratio R, and displacement V_t.

Next, recall that η_{ch} and $\eta_{fc,i}$ are assumed in Section 3.2 to depend only upon the compression ratio. Consequently, $B = B(r)$ which implies that the cylinder bore is a characteristic dimension under these conditions. To illustrate this dependence, Table 1 presents the results of several computations with an initial temperature and pressure of 300 K and 1 atm while the engine is assumed to operate at an equivalence ratio of 0.5.

In Table 1, the cylinder bore decreases with compression ratio. This result is a consequence of the charging and fuel conversion efficiencies increasing with the compression ratio (Fig. 3). That is, increasing the compression ratio causes the fuel conversion efficiency to increase and therefore permits a smaller engine to deliver the same power—an intuitive result.

Additionally, Fig. 3 indicates that despite the many crude approximations employed, the overall fuel conversion efficiency prediction is reasonably accurate for the smallest commercially available engine. One should also note that the generally low fuel conversion efficiency is attributable to poor charging efficiency—a well-known characteristic of two-stroke engines.

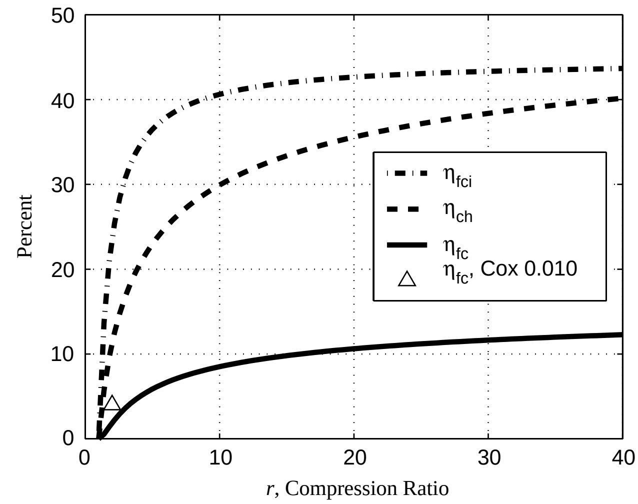

Fig. 3. The dependence of the charging and fuel conversion and efficiencies upon the compression ratio and comparison to the Cox 0.010 Glow-Ignition Model Airplane engine (Yang, 2000). Note that $\eta_{fc} = \eta_{fc,i} \eta_{\mathrm{ch}} \eta_m$ and that $\eta_m = 0.70$.

4.2. Intake conditions and power density

We now proceed to investigate the influence of the intake conditions on the cylinder bore. Rather than consider each parameter i.e., T_i, P_i, and Φ, separately, their combined effect on engine performance is investigated by defining an "intake parameter" viz.,

$$\zeta = \frac{\rho_i}{\rho_o} \Phi = \left(\frac{P_i}{P_o}\right)\left(\frac{T_o}{T_i}\right) \Phi, \qquad (18)$$

where ρ_o is the density of air at 300 K and 1 atm. Hence this parameter represents the properties of the fresh charge relative to a stoichiometric mixture at ambient conditions; a convenience because $\zeta = 1.0$ is a maximum value for non-supercharged HCCI engines. Whereas $\zeta = 0.5$ is typical for HCCI engines because the fresh charge is usually preheated and very lean mixtures are employed. One should note however, that ζ has little if any, physical significance outside the context of performance estimation.

Next, the cylinder bore is plotted in Fig. 4 versus ζ and the compression ratio r. Immediately, one notices that the cylinder bore is minimized when both the compression ratio and ζ are maximized. The relationship between compression ratio and cylinder bore was already discussed in Section 4.1. On the other hand, ζ captures the effect of charge density. That is, the mass of fuel burned and hence the work obtained from each cycle increases with ζ. Therefore, increasing ζ allows one to increase the power output of a given engine or substitute a smaller engine in its place.

The relationships between r, ζ, and the cylinder bore are important results because to be consistent with the overall

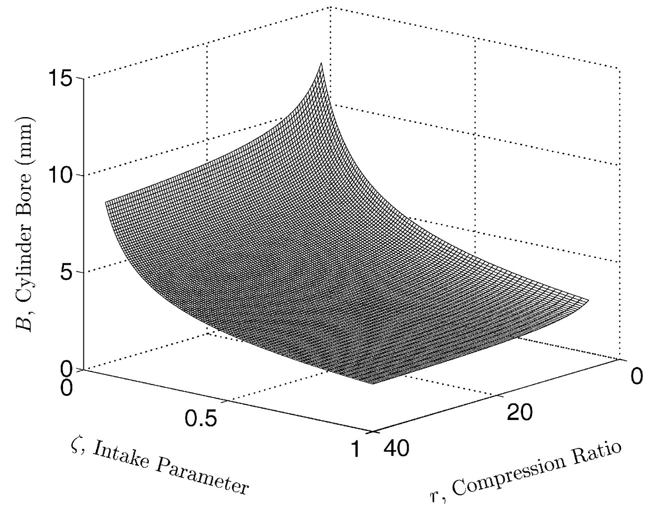

Fig. 4. The cylinder bore dependence upon the compression ratio and intake conditions for a non-supercharged 10 W engine. $\zeta = 1.0$ corresponds to $P_i = 1$ atm, $T_i = 300$ K, and $\Phi = 1.0$.

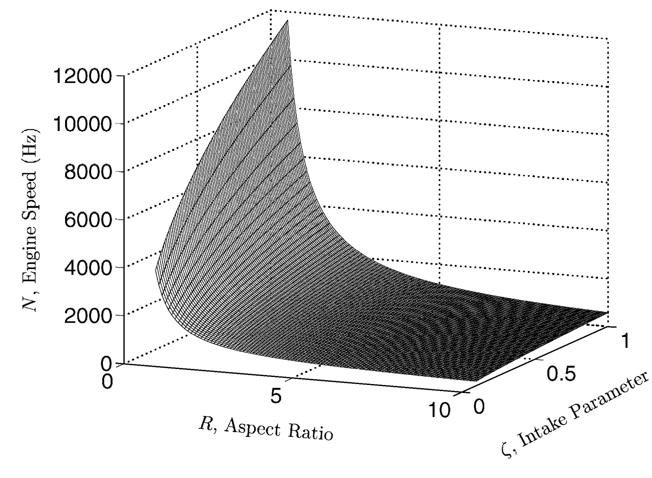

Fig. 5. The engine speed dependence upon the aspect ratio and intake conditions for a 10 W engine, $r = 25$. $\zeta = 1.0$ corresponds to $P_i = 1$ atm, $T_i = 300$ K, and $\Phi = 1.0$.

objective of battery replacement, maximizing the power density

$$P_d = \frac{P}{V_t} = \frac{4P}{\pi S B^2}, \tag{19}$$

is a goal. Consequently, for fixed power output and stroke, maximizing the power density is equivalent to minimizing the cylinder bore and thus maximizing both r and ζ.

According to Fig. 4, the power density can be increased without bound; obviously, there are limits. For instance, preheating the fresh charge i.e., $T_i > 300$ K, and using lean mixtures are frequent requirements for HCCI engines; both decrease ζ. Although, these requirements may be offset to some extent by supercharging i.e., $P_i > 1$ atm. The degree to which this can be done however, is constrained by peak cylinder pressures. Moreover, sealing becomes increasingly difficult when the compression ratio is increased and Fig. 3 may differ from an HCCI process; the latter possibility is investigated in the second paper.

4.3. Estimating the engine speed

Thus far, the compression ratio and intake parameter have been shown to be important parameters. We now consider the engine speed. According to Eq. (12), it depends upon the compression ratio, mean piston speed, total volume, and stroke-to-bore aspect ratio; but simplification yields

$$NB = \frac{\bar{U}_p}{2R}. \tag{20}$$

Again, the cylinder bore is prominent. Further manipulation gives

$$N = \frac{\bar{U}_p^{3/2}}{2R}\left[\frac{\pi \eta_m F_s e_c \rho_o \zeta}{8P} \cdot \frac{1}{\eta_{\text{ch}} \eta_{fc,i}}\right]^{1/2}. \tag{21}$$

One may infer from Fig. 3 however, that the product $\eta_{\text{ch}}\eta_{fc,i}$ varies from approximately 0.12 to 0.2. Consequently, the compression ratio dependence is weak and $N \approx N(R, \zeta)$ when power output is fixed. Hence the engine speed is plotted in Fig. 5 with $r = 25$ assumed. The engine speed depends strongly upon the aspect ratio, R. Hence one may conclude that the speed is essentially determined by the aspect ratio in this analysis.

4.4. Engine designs for fixed operating conditions

After exploring the influence of compression ratio, intake parameter, and aspect ratio separately, we now consider combinations of these parameters. To do this, we fix the intake parameter and obtain families of engine designs that deliver 10 W.

For example, consider propane-fueled engines with $\Phi = 0.5$, $T_i = 500$ K, and $P_i = 1$ atm ($\zeta = 0.3$). Assuming that the compression ratio and the aspect ratio are free variables, Eqs. (11) and (12) are used to generate the displacement and speed "maps" depicted in Figs. 6 and 7. Specific engine designs are then obtained by choosing a compression ratio and an aspect ratio.

To illustrate, several engine designs are presented in Table 2. Note that even though the bore is independent of aspect ratio, two types of engines are apparent: "small and fast" (large r, small R) and "big and slow" (small r, large R). To maximize power density, the former variety are preferred.

Performance estimation gives valuable guidance regarding the selection of key design parameters, but a fundamental question has been neglected: Can an HCCI engine operate within an entire design map such as Fig. 6? Intuitively, one would expect not. Consequently, the objective of the second paper is to identify regions in the compression ratio–aspect ratio space where operating conditions and HCCI are compatible.

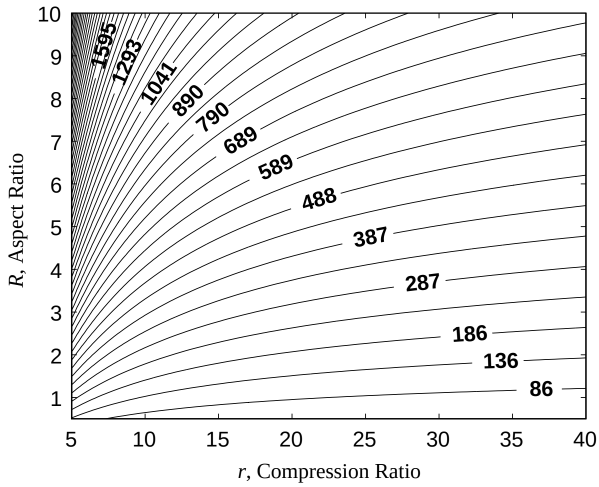

Fig. 6. Total cylinder volume, V_t (mm^3) required to deliver 10 W when operating with a mixture of propane and air, $\Phi = 0.5$, $T_i = 500$ K and $P_i = 1$ atm ($\zeta = 0.3$).

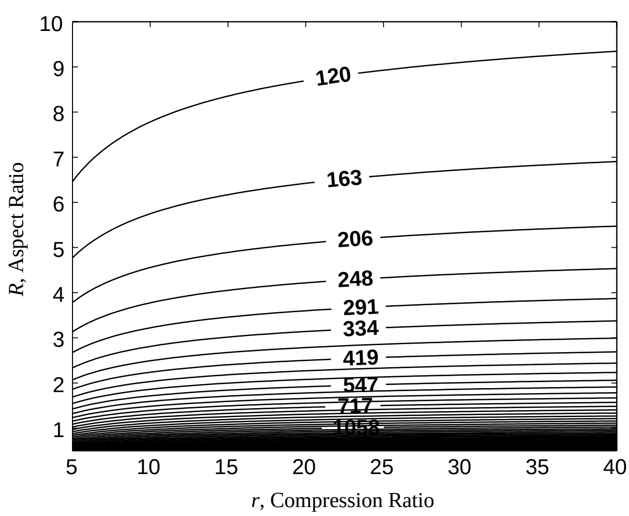

Fig. 7. Engine speed, N (Hz) required to deliver 10 W when operating with a mixture of propane and air, $\Phi = 0.5$, $T_i = 500$ K and $P_i = 1$ atm ($\zeta = 0.3$).

4.5. Small-scale considerations

In addition to neglecting design–HCCI compatibility, consequences of small engine dimensions have been overlooked. In the context of micro-combustion, these effects are primarily enhanced heat and mass transfer rates. Greater heat transfer rates are hypothesized to have two adverse effects on an HCCI engine: (1) decrease the effectiveness of compressive heating, and (2) decrease the indicated fuel conversion efficiency. The effect of enhanced mass transfer rates however, is unclear. That is, radicals can be destroyed or produced on walls depending upon surface properties; resulting in totally opposite effects. Further investigation of heat and mass transfer rates are left to the second paper.

Table 2
Representative engine designs depicted in Figs. 6 and 7

Compression ratio, r	Aspect ratio, R	V_t (mm^3)	N (Hz)	B (mm)
10	5	662	188	5.33
10	10	1324	94	5.33
35	1	73	1113	4.49
35	8	587	139	4.49

Although heat and mass transfer effects are strictly beyond the scope of the present analysis, one can infer favorable design conditions using geometry. According to Eq. (1), the surface-area-to-volume ratio is the relevant parameter. Referring to Fig. 2,

$$r = \frac{L}{c} \tag{22}$$

and the surface-area-to-volume ratio is given by

$$\frac{A_s}{\tilde{V}} = \frac{2}{L} + \frac{4}{B}. \tag{23}$$

The clearance distance c, and the stroke however are related by

$$c = \frac{S}{r-1}. \tag{24}$$

Next, using Eqs. (22), (24), and (7), the total combustion chamber volume becomes

$$V_t = \frac{\pi r S^3}{4R^2(r-1)} \tag{25}$$

and substitution of Eqs. (22), (24), (7) and (25) into Eq. (23) and simplification yields

$$\frac{A_s}{\tilde{V}} = \left(\frac{\pi}{V_t}\right)^{1/3} \left\{ \frac{2(r-1) + 4(rR)}{4^{1/3}(rR)^{2/3}(r-1)^{1/3}} \right\}. \tag{26}$$

Finally, Eqs. (7), (8), and (10) are used to further simplify Eq. (26). Rearrangement yields

$$\Psi(r,R) = B\frac{A_s}{\tilde{V}} = \left\{ \frac{2(r-1)}{rR} + 4 \right\}, \tag{27}$$

which is essentially a non-dimensional surface-area-to-volume ratio function.

According to Eq. (1), the specific heat transfer rate is minimized when Ψ is minimized. Inspection of Fig. 8 reveals that this occurs when *large* aspect ratios are employed. Also, Fig. 8 suggests that the compression ratio dependence is weak. In contrast, *small* aspect ratios maximize power density (Section 4.2). Therefore, minimizing heat transfer and maximizing power density are opposing objectives.

Lastly, the degree to which heat transfer can be decreased by large aspect ratios is limited. That is, Eq. (27) has a minimum value of 4, and Ψ is within 5% of this limit when

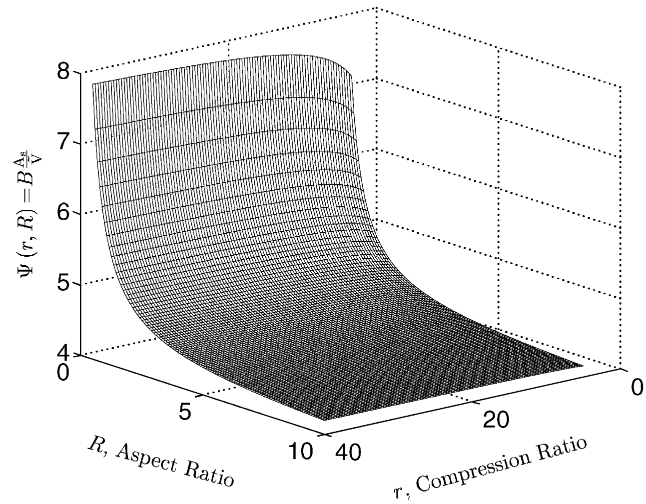

Fig. 8. Non-dimensional surface-area-to-volume ratio function, Eq. (27).

the aspect ratio is 10. Thus, aspect ratios greater than 10 offer almost no benefit.

5. Conclusion

This paper has presented a concept for a 10 W miniature free-piston engine-compressor and various considerations for its design. Specific results are summarized as follows:

- *Combustion mode*. In small scales, traditional engine combustion schemes are generally infeasible due to quenching effects; HCCI is a promising alternative.
- *Compression ratio*. The nominal compression ratio for this engine is a crucial parameter because it determines the compression history of the charge, affects the fuel conversion efficiency, and establishes the engine size. On the other hand, it affects neither the engine speed nor the specific heat transfer rate. Also, HCCI does not have a fundamental compression ratio limitation like SI. Consequently, the compression ratio may be increased virtually without bound. Practically however, sealing and material properties will impose limits.
- *Aspect ratio*. The performance analysis revealed that for a crankshaft-equipped engine, the stroke-to-bore aspect ratio establishes the engine speed. Additionally, the aspect ratio essentially determines the surface-area-to-volume ratio. More significantly however, *small* aspect ratios were found to maximize power density while *large* aspect ratios were found to minimize heat transfer. Consequently, a compromise must be sought between maximizing power density and minimizing heat transfer rates. Also, essentially no further reduction in heat transfer may be achieved with aspect ratios greater than 10.

Finally, HCCI depends strongly upon engine operation and design. Small scales are expected to impose additional constraints. Consequently, the next step is to investigate these aspects in detail.

Notation

A_B	bounce chamber area, Eq. (2), m^2
A_C	combustion chamber area, Eq. (2), m^2
A_{cp}	compressor area, Eq. (2), m^2
A_s	surface area, Eq. (1), m^2
A_{sc}	scavenge pump area, Eq. (2), m^2
$A_s/\tilde{V}$	surface area to volume ratio, Eq. (1), 1/m
B	cylinder bore, Eq. (7), mm
c	clearance distance, Eq. (22), mm
D_s	scavenge pump displacement volume, Eq. (15), m^3
e_c	lower heating value of fuel, Eq. (3), kJ/kg
F	fuel–air ratio (mass basis), dimensionless
F_s	stoichiometric fuel–air ratio (mass basis), Eq. (4), dimensionless
F_x	x-direction force, Eq. (2), N
L	combustion chamber height, Eq. (22), mm
m	mass of material, Eq. (1), kg
$\dot{m}_a$	mass flow rate of air, Eq. (4), kg/s
$\dot{m}_f$	mass flow rate of fuel, Eq. (3), kg/s
m_p	piston mass, Eq. (2), kg
N	engine speed, Eq. (5), Hz
N_s	scavenge pump speed, Eq. (15), Hz
P	delivered or brake power, Eq. (3), W
P_1	transfer port pressure, Eq. (15), atm
P_B	bounce chamber pressure, Eq. (2), atm
P_C	combustion chamber pressure, Eq. (2), atm
P_{cp}	compressor pressure, Eq. (2), atm
P_d	power density, Eq. (19), W/cm^3
P_e	exhaust port pressure, Eq. (15), atm
P_i	intake pressure, atm
P_{sc}	scavenge pump pressure, Eq. (2), atm
P_o	normal pressure of air, Eq. (18), 1 atm
$\dot{q}$	heat transfer rate per unit mass, W/kg
$\dot{q}''$	heat flux, Eq. (1), W/m^2
$\bar{\dot{q}}''$	average heat flux, Eq. (1), W/m^2
$\dot{Q}$	heat transfer rate, Eq. (1), W
r	compression ratio ($r = V_t/V_c$), Eq. (9), dimensionless
R	stroke to bore aspect ratio, $R = S/B$, Eq. (7), dimensionless
S	piston stroke, Eq. (6), m
T_1	transfer port temperature, Eq. (15), K
T_i	intake temperature, Eq. (15), K
T_o	normal temperature of air, Eq. (18), 300 K
$\bar{U}_p$	mean piston speed, Eq. (6), m/s
V_c	cylinder clearance volume ($=\pi B^2 c/4$), Eq. (9), mm^3
V_d	displaced volume ($=\pi B^2 S/4$), Eq. (5), mm^3
V_t	total cylinder volume ($=\pi B^2 L/4$), Eq. (10), mm^3
$\tilde{V}$	volume, Eq. (1), m^3
x	Cartesian coordinate, Eq. (2), m

Greek letters

α	air-standard Otto cycle adjustment factor (=0.6), Eq. (13)

γ specific heat ratio used in adjusted air-standard Otto cycle (=1.3), Eq. (13)
ζ intake parameter ($=\rho_i/\rho_o\Phi$), Eq. (18), dimensionless
η_{ch} charging efficiency (=mass of fresh charge retained/reference mass), dimensionless
η_{fc} engine fuel conversion efficiency, Eq. (3), dimensionless
$\eta_{fc,i}$ fuel conversion efficiency of the engine cycle, dimensionless
η_m mechanical efficiency, dimensionless
η_{tr} trapping efficiency (=mass of fresh charge trapped/mass of fresh charge delivered), dimensionless
η_v engine volumetric efficiency, ($=m_a/\rho_i V_d$), Eq. (5), dimensionless
$\eta_{v,s}$ scavenge pump volumetric efficiency, Eq. (15), dimensionless
Λ delivery ratio (=mass of fresh charge delivered/reference mass), dimensionless
ρ density, Eq. (1), kg/m^3
ρ_i density of air at the intake, Eq. (5), kg/m^3
$\bar{\rho}$ average density, Eq. (1), kg/m^3
ρ_o density of air at 300 K and 1 atm, Eq. (18), kg/m^3
Φ fuel–air equivalence ratio ($=F/F_s$), $\Phi < 1$, fuel-lean; $\Phi > 1$, fuel-rich; Eq. (4), dimensionless
Ψ non-dimensional surface-area-to-volume ratio ($\Psi(r,R) = BA_s/\tilde{V}$), Eq. (27)

Acknowledgements

This project was sponsored by Honeywell International under DARPA Contract no. F30602-99-C-0200.

References

Allen, M., et al. (2001). *Research topics–miniature MEMS free-piston engine generator*. Georgia Institute of Technology Internet Document (Last loaded July 2001). URL http://comblab5.ae.gatech.edu/Minipiston/intro.htm

Aoyama, T., Hattori, Y., & Mizuta, J. (1996). *An experimental study on premixed-charge compression ignition gasoline engine*. SAE Technical Paper 960081.

Chen, Z., Konno, M., Oguma, M., & Yani, T. (2000). *Experimental study of CI natural-gas/DME homogeneous charge engine*. SAE Technical Paper 2000-01-0329.

Christensen, M., Hultqvist, A., & Johansson, B. (1999). *Demonstrating the multi fuel capability of a homogeneous charge compression ignition engine with variable compression ratio*. SAE Technical Paper 1999-01-3679.

Christensen, M., & Johansson, B. (1998). *Influence of mixture quality on homogeneous charge compression ignition*. SAE Technical Paper 982454.

Christensen, M., & Johansson, B. (1999). *Homogeneous charge compression ignition with water injection*. SAE Technical Paper 1999-01-0182.

Christensen, M., Johansson, B., AmnJus, P., & Mauss, F. (1998). *Supercharged homogeneous charge compression ignition*. SAE Technical Paper 980787.

Christensen, M., Johansson, B., & Einwall, P. (1997). *Homogeneous charge compression ignition (HCCI) using isooctane, ethanol, and natural gas-a comparison with spark ignition operation*. SAE Technical Paper 972874.

Disseau, M. L. D. S., et al. (2000). *Investigation of combustion processes in small aspect ratio combustors*. Georgia Institute of Technology Internet Document (Last loaded August 2000). URL http://comblab5.ae.gatech.edu/Minipiston/ConstVol.htm

Epstein, A. H., Senturia, S. D., Anathasuresh, G., Ayon, A., Breuer, K., Chen, K., Ehrich, F. E., Gauba, G., Ghodssi, R., Groshenry, C., Jacobson, S., Lang, J. H., Lin, C., Mehra, A., Miranda, J. M., Nagle, S., Orr, D. J., Piekos, E., Schmidt, M. A., Shirley, G., Spearing, M. S., Tan, C. S., Tzeng, Y., Waitz, I. A. (1997). Power MEMS and microengines. In *Transducers '97 Chicago*: *Digest of technical papers* (pp. 753–756), June 16–19, 1997. Chicago, IL: IEEE.

Fernandez-Pello, C., Liepmann, D., & Pisano, A., et al. (2001). *MEMS rotary combustion laboratories*. University of California at Berkeley Internet Document (Last loaded July 2001). URL http://www.me.berkeley.edu/mrcl/

Flowers, D., Aceves, S., Smith, R., Torres, J., Girard, J., & Dibble, R. (2000). *HCCI in a CFR engine*: *Experiments and detailed kinetic modeling*. SAE Technical Paper 2000-01-0328.

Galileo Research Inc. (2001). *Free-piston engine-generator technology*. Internet Document (Last loaded September 2001). URL http://www.galileoresearch.com/FPEG_Technology/peg_technology.htm

Gentili, R., Frigo, S., Tognotti, L., Patrice, H., & Lavy, J. (1997). *Experimental study on ATAC (Active Thermo-Atmosphere Combustion) in a two-stroke gasoline engine*. SAE Technical Paper 970363.

Goldsborough, S. S., & Van Blarigan, P. (1999). *A numerical study of a free piston IC engine operating on homogeneous charge compression ignition combustion*. SAE Technical Paper 990619.

Gray III, A., & Ryan III, T. W. (1997). *Homogeneous charge compression ignition (HCCI) of diesel fuel*. SAE Technical Paper 971676.

Hagendorf, U., Janicke, M., Schüth, F., Schubert, K., & Fichtner, M. (1998). A Pt/Al_2O_3 coated microstructured reactor/heat exchanger for the controlled H_2/O_2-reaction in the explosion regime. In *Process miniturization: Second international conference on microreaction technology* (pp. 81–87). New Orleans, LA: The American Institute of Chemical Engineers.

Heywood, J. B. (1988). *Internal combustion engine fundamentals*. New York: McGraw-Hill.

Heywood, J. B., & Sher, E. (1999). *The two-stroke cycle engine*: *Its development*, *operation*, *and design*. Warrendale, PA: Society of Automotive Engineers.

Hsing, I. M., Srinivasan, R., Harold, M. P., Jensen, K. F., & Schmidt, M. A. (2000). Simulation of micromachined chemical reactors for heterogeneous partial oxidation reactions. *Chemical Engineering Science*, *55*(1), 3–13.

Hultqvist, A., Christensen, M., Johansson, B., Franke, A., Richter, M., & Alden, M. (1999). *A study of the homogeneous charge compression ignition combustion process by chemiluminescent imaging*. SAE Technical Paper 1999-01-3680.

Iida, N. (1994). *Combustion analysis of methanol-fueled active thermo-atmosphere combustion (ATAC) engine using a spectroscopic observation*. SAE Technical Paper 940684.

Iwabuchi, Y., Kawai, K., Shoji, T., & Takeda, Y. (1999). *Trial of new concept diesel combustion system-premixed compression-ignited combustion*. SAE Technical Paper 1999-01-0185.

Jensen, K. F. (1999). Microchemical systems: Status, challenges and opportunities. *A.I.Ch.E. Journal*, *45*(10), 2051–2054.

Knobloch, A. et al. (2000). *MEMS rotary combustion laboratories*. University of California at Berkeley Internet Document (Last loaded August 2000). URL http://euler.me.berkeley.edu/mrcl/

Lavy, J., Duret, P., Habert, P., Esterlingot, E., & Gentili, R. (1996). Investigation on controlled auto-ignition combustion (A.T.A.C.) in two-stroke gasoline engine. In Selected presentations from the *Second international workshop and thematic network meeting on modernised 2/stroke engines* (5th ed.), 3-4 July 1996. Manchester, UK: The 2/Stroke Thematic Network Circular.

Najt, P. M., & Foster, D. E. (1983). *Compression-ignited homogeneous charge combustion*. SAE Technical Paper 830264.

Onishi, S., Jo, S. H., Shoda, K., Jo, P. D., & Kato, S. (1979). *Active thermo-atmosphere combustion (ATAC)—a new combustion process for internal combustion engines*. SAE Technical Paper 790501.

Oppenheim, A. K. (1984). *The knock syndrome-its cures and its victims*. SAE Technical Paper 841339.

Oppenheim, A. K., & London, A. L. (1950). *The free-piston gas generator: A thermodynamic-dynamic analysis*. Technical Report, Stanford University, Report FP-1, Navy Contract N6-ONR-251 Task Order 6.

Peterson, R. B. (2001). Small packages. *Mechanical Engineering*, *123*(6), 58–61.

Quiram, D. J., Hsing, I., Franz, A. J., Jensen, K. F., & Schmidt, M. A. (2000). Design issues for membrane-based, gas phase microchemical systems. *Chemical Engineering Science*, *55*(16), 3065–3075.

Quiram, D. J., Hsing, I., Franz, A. J., Srinivasan, R., Jensen, K. F., & Schmidt, M. A. (1998). Characterization of microchemical systems using simulations. In *Process miniturization: Second international conference on microreaction technology* (pp. 205–210). New Orleans, LA: The American Institute of Chemical Engineers.

Richter, M., Franke, A., Alden, M., Hultqvist, A., & Johansson, B. (1999). *Optical diagnostics applied to a naturally aspirated homogeneous charge compression ignition engine*. SAE Technical Paper 1999-01-3649.

Ryan III, T. W., & Callahan, T. J. (1996). *Homogeneous charge compression ignition of diesel fuel*. SAE Technical Paper 961160.

Srinivasan, R., Hsing, I., Berger, P. E., Jensen, K. F., Firebaugh, S. L., & Schmidt, M. A., et al. (1997). Micromachined reactors for catalytic partial oxidation reactions. *A.I.Ch.E. Journal*, *43*(11), 3059–3069.

Stanglmaier, R. H., & Roberts, C. E. (1999). *Homogeneous charge compression ignition (HCCI): Benefits, compromises, and future engine applications*. SAE Technical Paper 1999-01-3682.

Taylor, C. F. (1985). *The internal combustion engine in theory and practice: Thermodynamics, fluid flow, performance*, Vol. I. Cambridge, MA: MIT Press.

Thring, R. H. (1989). *Homogeneous-charge compression ignition (HCCI) engines*. SAE Technical Paper 892068.

Van Blarigan, P., Paradiso, N., & Goldsborough, S. S. (1998). *Homogeneous charge compression ignition with a free piston: A new approach to ideal Otto cycle performance*. SAE Technical Paper 982484.

Waitz, I. A., Gauba, G., & Tzeng, Y. (1998). Combustors for micro-gas turbine engines. *Journal of Fluids Engineering*, *120*(1), 109–117.

Yang, W. (2000). Personal communication.

Yang, W., Bonne, U., & Johnson, B. R. (2001). *Microcombustion engine/generator*. U.S. Patent 6,276,313.

Yang, W. et al. (1999). *MEMS free-piston knock engine*. Technical Proposal, DARPA Contract F30602-99-C-0200, Honeywell Technology Center, 12001 State Highway 55, Plymouth, MN 55441.